Basic Study on Regenerative Air Brake Using Observer-based Thrust Control for Electric Airplane

Kentaro Yokota, Hiroshi Fujimoto, and Yoichi Hori

The University of Tokyo

5-1-5, Kashiwanoha, Kashiwa, Chiba, 277-8561, Japan

Phone: +81-4-7136-3881

Email: yokota.kentaro19@ae.k.u-tokyo.ac.jp, fujimoto@k.u-tokyo.ac.jp, hori@k.u-tokyo.ac.jp

Abstract—Research and development have been very active in electric airplanes (EAs). EAs use electric motors as the power source; therefore, EAs are expected to achieve more secure, more efficient, and more eco-friendly aviation. The conventional airplanes use mechanic air brakes such as spoilers to adjust the descent angle; however, they are difficult to control even for a skilled pilot. Previous research showed that electric motors enable EAs to regenerate their potential energy while descending as the windmilling propeller produces negative torque and thrust. This negative thrust works as a substitute air brake, called regenerative air brake. This paper proposes the thrust control method of regenerative air brake for automatic descent. Furthermore, the observer-based thrust estimation method is also proposed since adding force sensors decreases the stiffness of the thrusters. The effectiveness of the proposed method is verified by simulations and experiments in the wind tunnel.

Index Terms—Electric airplane, electric motor, regeneration power, regeneration energy, propeller

I. INTRODUCTION

A. Electric Airplane

Over the past few years, the demand for personal and eco-friendly aviation has increased. Accordingly, several studies have been conducted on electric airplanes (EAs) [1]. As EAs are powered by electric motors, they have the following advantages:

1) Motor torque generation is 100 times faster than that of internal combustion engines [2].
2) Motor torque measurement is accurate [2].
3) Distributed installation and independent control of motors are easy [3].
4) Power regeneration is possible [4].

These advantages enable EAs to be more secure, more efficient, and more eco-friendly aviation.

The authors' research group has proposed a quick thrust control method [5] and range extension systems [6] [7] by adopting the motion control theories developed in the automotive industry [8].

B. Power Regeneration by Propellers

Previous studies showed that the windmilling propeller allows the motor to generate electric power [9] [10] [4] [11] [12]. A propeller in the windmill state produces negative thrust and negative torque; therefore, EAs regenerate about 10% of their potential energy while descending [4]. Additionally,
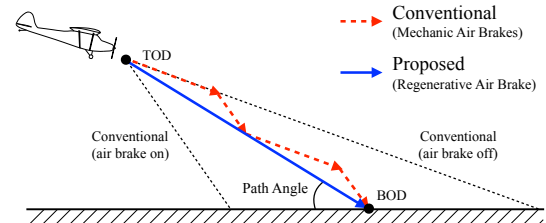
Fig. 1. The conventional and proposed descent routes [9].

the energy generated during descent allows an EA to cruise about 60% of the descent distance at most, according to [12]. Regeneration during descent reduces the batteries for the descent, loiter, go-around, and taxiing.

C. Regenerative Air Brake

This paper focuses on the control of the descending airplane. The conventional method uses mechanic air brakes such as spoiler to adjust the descent angle; however, since they cannot be controlled continuously, even a skilled pilot finds it difficult to operate the brakes [9]. The airfield usually requests the top of descent (TOD) and the bottom of descent (BOD), but due to this difficulty, the conventional airplane descends a zigzag path, as shown in Fig. 1.

The idea of regenerative air brake suggests the negative thrust of the windmilling propeller can substitute the conventional mechanic air brakes [11]. Compared to mechanic air brakes, regenerative air brake does not require additional actuators and has a better control performance.

In [11], the method of descent using regenerative air brake was proposed and demonstrated in the flight tests. In this method, the controller gives the input torque command on a feedforward basis, leading to poor robustness. In addition, the adjustment of the descent angle still depends on the ability of the pilot since the pilot can only change the input torque. In order to achieve a better performance of descent control, the propeller thrust should be controlled. Previous research on force control of rotors includes [5] and [13].

D. About This Paper

The lift, weight, drag, and thrust determines the descent angle of an airplane. If the airspeed is constant, the thrust is

Parameter	Definition	Unit
β	propeller pitch angle	rad
γ	descent angle of airplane	rad
ρ	air density	$\mathrm{kg\,m^3}$
n	rotational speed of propeller	rps
B_ω	viscosity coefficient of motor	$\mathrm{N\,m\,s\,rad^{-1}}$
C_D	drag coefficient of airplane	–
C_F	thrust coefficient of propeller	–
C_L	lift coefficient of airplane	–
C_Q	torque coefficient of propeller	–
D	drag of airplane	N
D_p	propeller diameter	m
F	propeller thrust	N
J	advance ratio	–
J_ω	inertia moment of propeller	$\mathrm{kg\,m^2}$
L	lift of airplane	N
M	mass of airplane	kg
P	input power of motor	W
Q	counter torque of propeller	N m
S	wing area	$\mathrm{m^2}$
T	input toque of motor	N m
T_C	coulomb friction of motor	N m
V	airspeed	$\mathrm{m\,s^{-1}}$

the only factor that changes the angle. Hence, it is crucial to control the propeller thrust to keep the desired descent angle.

The purpose of this study is to achieve negative thrust control in the regenerative area. The proposed method consists of three steps.

Step 1 is the observer-based quick airspeed estimation. The conditions of regeneration vary depending on airspeed, but the pitot tube has poor responsiveness. The airspeed must be quickly estimated.

Step 2 is the observer-based thrust estimator. The existing airplanes do not have force sensors on propellers, and adding such sensors degrade the stiffness of the thrusters. Therefore, the propeller thrust cannot be measured and should be estimated.

Step 3 is the negative thrust control method. By using Step 1 and Step 2, the negative thrust controller is designed.

The negative thrust control enables EAs to achieve more robust descent and higher followability to the target route. The descent routes of the conventional method using mechanic air brakes and the proposed method using regenerative air brake are shown in Fig. 1.

Table I shows the definitions of the plant parameters in this paper.

II. MODELING OF SINGLE MOTOR ELECTRIC AIRPLANE

In this section, a single motor EA is modeled.

A. Airplane Dynamics [10]

Fig. 2(a) shows a view of the airplane in a steady descent. The vector sum of all forces is zero since the airplane is in equilibrium. Hence, in the direction of descent,

$$F \cos \delta + Mg \sin \gamma - D = 0. \tag{1}$$

Normal to this direction,

$$L + F \sin \delta - Mg \cos \gamma = 0. \tag{2}$$

These equations can be solved for γ to give

$$\tan \gamma = \frac{D - F \cos \delta}{L + F \sin \delta}. \tag{3}$$

L and D are given by

$$L = \frac{1}{2} \rho C_L S V^2, \tag{4}$$

$$D = \frac{1}{2} \rho C_D S V^2. \tag{5}$$

L and D are constant under constant ρ and V; therefore, γ becomes a function of only F. Also, from (3), the negative F allows a wide range of γ.

B. Propeller Dynamics [10], [14]

A propeller-driven airplane gets all of its thrust from the propeller. Fig. 2(b) shows velocities and forces acting on the propeller blade element. V_i is the induced velocity, $\mathrm{d}L$ is the differential lift, and $\mathrm{d}D$ is the differential drag. The contribution of the blade element to F and Q is

$$\mathrm{d}F = \mathrm{d}L \cos (\phi + \alpha_i) - \mathrm{d}D \sin (\phi + \alpha_i), \tag{6}$$

$$\mathrm{d}Q/r = \mathrm{d}L \sin (\phi + \alpha_i) + \mathrm{d}D \cos (\phi + \alpha_i). \tag{7}$$

Similar to (4) and (5), dL and dD can be calculated by

$$\mathrm{d}L = \frac{1}{2} \rho C_L c \mathrm{d}r W^2, \tag{8}$$

$$\mathrm{d}D = \frac{1}{2} \rho C_D c \mathrm{d}r W^2, \tag{9}$$

where c is the chord. Let B be the number of the blades, then

$$
\begin{aligned}
F &= B \int \mathrm{d}F \\
&= B \int \{\mathrm{d}L \cos (\phi + \alpha_i) - \mathrm{d}D \sin (\phi + \alpha_i)\}, \tag{10}
\end{aligned}
$$

$$
\begin{aligned}
Q &= B \int \mathrm{d}Q \\
&= B \int r \{\mathrm{d}L \sin (\phi + \alpha_i) + \mathrm{d}D \cos (\phi + \alpha_i)\}. \tag{11}
\end{aligned}
$$

Considering the theoretical equations (8) – (11), C_F and C_Q are defined from experimental results as follows:

$$C_F = \frac{F}{\rho n^2 D_p^4}, \tag{12}$$

$$C_Q = \frac{Q}{\rho n^2 D_p^5}. \tag{13}$$

From Fig. 2(b), the angle of resultant flow ϕ is determined by the ratio of V and $2\pi nr$.

$$\tan \phi = \frac{V}{2\pi nr} = \frac{J}{\pi \frac{2r}{D_p}}. \tag{14}$$

J is defiend by

$$J = \frac{V}{nD_p}. \tag{15}$$
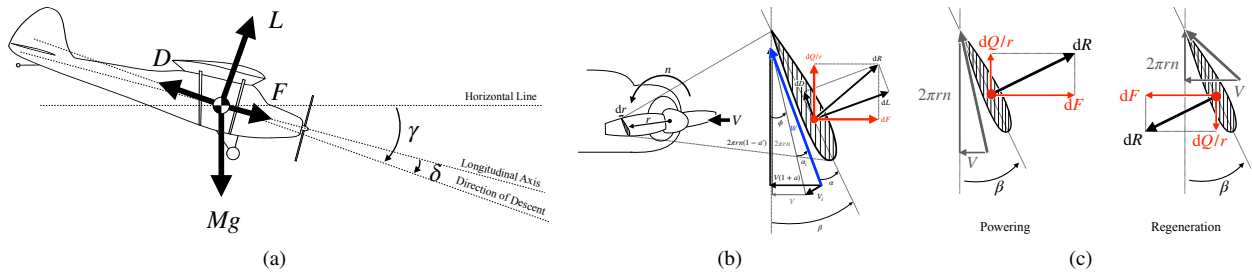
Fig. 2. (a) A view of the airplane in a steady descent. (b) Velocities and forces acting on the propeller blade element. (c) A view of the powering propeller (left) and windmilling propeller (right).

Thus, C_F and C_Q are functions of J. F and Q can be written as

$$F = C_F(J)\rho n^2 D_p^4, \qquad (16)$$

$$Q = C_Q(J)\rho n^2 D_p^5. \qquad (17)$$

Fig. 2(c) shows a view of the powering propeller (left) and windmilling propeller (right). As the figure shows, if the directions of F and Q are assumed to be positive when powering, the windmilling propeller produces negative F and Q. In other words, C_F and C_Q become negative at high J. n is small and V is large in the regenerative area; therefore, the conditions of regeneration are limited.

The equation of motion of the electric motor is

$$T - Q = 2\pi J_\omega \frac{\mathrm{d}n}{\mathrm{d}t} + 2\pi B_\omega n + T_C. \qquad (18)$$

Ignoring the friction of the motor in (18), P is calculated by

$$P = 2\pi nT = 2\pi nQ. \qquad (19)$$

P becomes negative when Q is negative, enabling power regeneration.

III. PROPOSAL OF NEGATIVE THRUST CONTROL USING OBSERVER-BASED THRUST ESTIMATOR

The proposed method consists of three steps. Step 1 is the observer-based airspeed estimation, Step 2 is the observer-based thrust estimator, and Step 3 is the negative thrust control.

A. Step 1: Observer-based Airspeed Estimation

The conditions of regeneration vary depending on airspeed, but the pitot tube has poor responsiveness. The time constant of the pitot tube on most airplanes is about a few seconds. In order to stay in the regenerative area, the airspeed must be quickly estimated. In Step 1, the observer-based airspeed estimation scheme is proposed by taking advantage of the quick response of electric motors.

The idea of airspeed estimation using motor torque is proposed in [15]; however, the motor friction is ignored, and the response time is not discussed. Since this study focuses on the regenerative area where the torque is small, the friction is not negligible. The propeller motor is precisely modeled, and the response time of the pitot tube and the proposed method is compared.

From (18), the counter torque observer is designed, as shown in Fig. 3(a). By using (15), (17), and the estimated value of Q, V can be estimated as follows:

$$\hat{V} = nD_p C_Q^{-1}\left(\frac{\hat{Q}}{\rho n^2 D_p^5}\right). \qquad (20)$$

B. Step 2: Observer-based Thrust Estimation

In order to control the descent angle, the thrust must be estimated since adding force sensors decreases the stiffness of the thrusters. In Step 2, the observer-based thrust estimator is proposed. The block diagram of the observer-based thrust estimator is shown in Fig. 3(b). As shown in Fig. 2(b), F and Q are produced from the same aerodynamic force; therefore, it is reasonable to estimate F from Q.

$C_F(J)$ and $C_Q(J)$ are approximated by a polynomial in the conventional modeling. However, as seen in Fig. 4(a) and Fig. 4(b), the relation between the advance ratio and the coefficients have significant errors due to the difference in Reynolds number.

The proposed modeling uses $C_Q - C_F$ relation. There are mainly two advantages of this model. The first advantage is that it has fewer errors due to the difference in Reynolds number, as shown in Fig. 4(c). The second advantage is that $C_Q - C_F$ can be linearly approximated in the regeneration area, as shown in Fig. 4(d). Thus,

$$C_F = aC_Q + b, \qquad (21)$$

$$\hat{F} = a\frac{\hat{Q}}{D_p} + b\rho n^2 D_p^4. \qquad (22)$$

In general, higher-order approximation gives a better fitting of the data. However, when the propeller is put in an untested area, the difference between the actual performance and the high order approximation could be significant. This is why the order of the approximation should be as low as possible, and this discovery of $C_Q - C_F$ linear relation is valuable. Regarding APC propeller 11×4, the maximum error of the conventional model is about 9%, but that of the proposed model is about 4%.

C. Step 3: Negative Thrust Control

The negative thrust must be controlled to keep the constant descent angle during power regeneration. In Step 3, the negative thrust controller is proposed using Step 1 and Step 2.
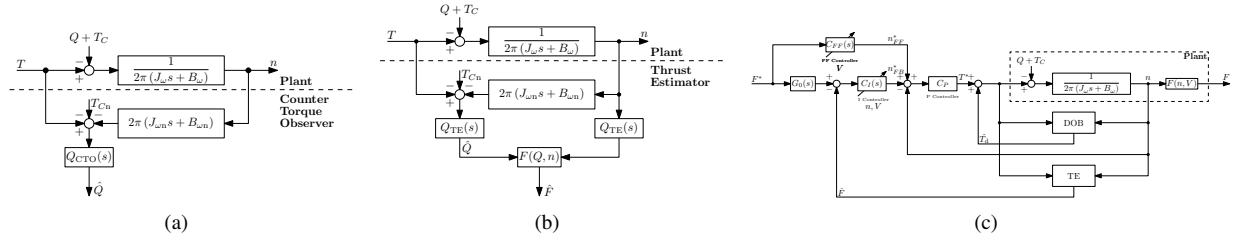
Fig. 3. (a) Step 1: Counter torque observer. (b) Step 2: Observer-based thrust estimator. (c) Step 3: Negative thrust controller.
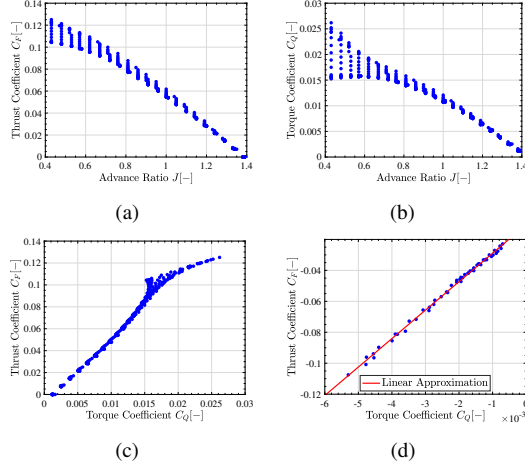
Fig. 4. (a) The relation between J and C_F of APC propeller 10×10 [16]. (b) The relation between J and C_Q of APC propeller 10×10 [16]. (c) The relation between C_Q and C_F of APC propeller 10×10 [16]. (d) The relation between C_Q and C_F of windmilling APC propeller 11×5.5 [4].

The negative thrust controller is designed as a two-degree-of-freedom control and uses the estimated thrust $\hat{F}$ in the feedback controller. Fig. 3(c) shows the block diagram of the controller.

1) Rotational Speed Controller: Firstly, the rotational speed controller is designed. The block diagram is shown in Fig. 5(a). The rotational speed controller is a proportional controller using the feedforward compensation by the disturbance observer shown in Fig. 5(b). In Fig. 5(b) the disturbance torque T_d is

$$T_\mathrm{d} = Q + 2\pi B_\omega n + T_C. \tag{23}$$

The nominal plant is

$$\frac{n}{T} = \frac{1}{2\pi J_{\omega \mathrm{n}} s}. \tag{24}$$

The proportional gain C_P is given by

$$\frac{n}{n^*} = \frac{C_P \frac{1}{2\pi J_{\omega \mathrm{n}} s}}{1 + C_P \frac{1}{2\pi J_{\omega \mathrm{n}} s}} = \frac{\omega_1}{s + \omega_1}. \tag{25}$$

2) Feedforward Controller: Secondly, the feedforward controller is designed. Applying quadratic approximation, $C_F(J)$ can be written as

$$C_F(J) = a_{CF} J^2 + b_{CF} J + c_{CF}. \tag{26}$$
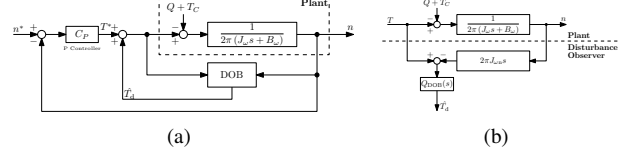
Fig. 5. (a) Rotational speed controller. (b) Disturbance observer.

From (15), (16), and (26),

$$F = \left(a_{CF} J^2 + b_{CF} J + c_{CF}\right) \rho n^2 D_p^4 \tag{27}$$

$$= \rho \left(a_{CF} V^2 D_p^2 + b_{CF} V D_p^3 n + c_{CF} D_p^4 n^2\right) \tag{28}$$

$$= f(n). \tag{29}$$

From (29),

$$F = f\left(\frac{n}{n^*} \cdot n^*\right). \tag{30}$$

Thus,

$$n^* = \frac{n^*}{n} \cdot f^{-1}(F) = \frac{s + \omega_1}{\omega_1} f^{-1}(F). \tag{31}$$

Since (31) is not proper, the feedforward controller is given by

$$n_{FF}^* = \frac{s + \omega_1}{\omega_1} f^{-1}(F) \frac{\omega_g}{s + \omega_g}. \tag{32}$$

$\frac{\omega_g}{s + \omega_g}$ is the reference model. The feedfoward controller is a nonlinear variable controller because $f(n)$ is also a function of V. V is given by Step 1.

3) Feedback Controller: Finally, the feedback controller is designed. The filter $G_0(s)$ is given as follows:

$$G_0(s) = \frac{\omega_g}{s + \omega_g}. \tag{33}$$

Taylor expansion of (29) at the operating point $n = n_0$ gives the first-order approximation of F,

$$F \approx a_F(n - n_0) + b_F, \tag{34}$$

where

$$a_F = b_{CF} V D_p^3 + 2 c_{CF} D_p^4 n_0, \tag{35}$$

$$b_F = a_{CF} V^2 D_p^2 + b_{CF} V D_p^3 n_0 + c_{CF} D_p^4 n_0^2. \tag{36}$$

The rotational speed controller is assumed to be fast enough to get $n = n^*$. The plant is assumed to be

$$\frac{\Delta F}{\Delta n^*} = \frac{\Delta F}{\Delta n} = a_F. \tag{37}$$

(a) (b)
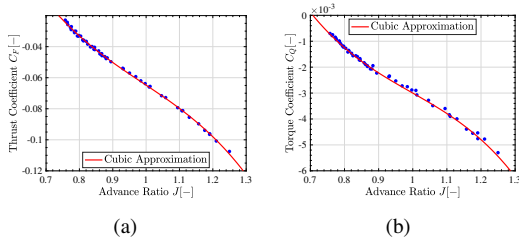
Fig. 6. (a) The relation between J and C_F of windmilling APC propeller 11×5.5 [4]. (b) The relation between J and C_Q of windmilling APC propeller 11×5.5 [4].
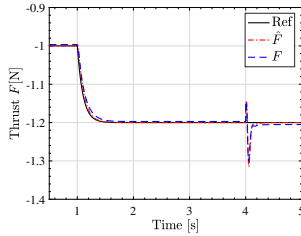
Fig. 7. The simulation result of step response and tailwind disturbance response.

The feedback controller is an integral controller and the gain C_2 is given by

$$\frac{F}{F^*} = \frac{C_I(s)a_F}{1 + C_I(s)a_F} = \frac{\frac{C_2}{s}a_F}{1 + \frac{C_2}{s}a_F} = \frac{\omega_2}{s + \omega_2}. \tag{38}$$

The feedback controller is a nonlinear variable controller because a_F is a function of n_0 and V. V is given by Step 1, and the output of Step 2 is used as the feedback.

IV. SIMULATION

A simulation verifies the proposed method in this section. The poles of each controller are as follows:

$$\omega_1 = 100\,\mathrm{rad\,s^{-1}}, \tag{39}$$
$$\omega_2 = 50\,\mathrm{rad\,s^{-1}}, \tag{40}$$
$$\omega_g = 50\,\mathrm{rad\,s^{-1}}. \tag{41}$$

The simulation model uses the parameter of APC propeller 11×5.5 propeller. The $J - C_F$ and $J - C_Q$ curves are shown in Fig. 6(a) and Fig. 6(b). B_ω and T_C are assumed to be zero in this simulation.

The step response and the tailwind disturbance response are shown in Fig. 7. $\hat{F}$ is the estimated thrust, which is controller feedback. F is the real value. V was set at $V = 7\,\mathrm{m\,s^{-1}}$. The thrust reference was exponentially changed from $-1\,\mathrm{N}$ to $-1.2\,\mathrm{N}$ at $t = 1\,\mathrm{s}$, and V was changed to $6\,\mathrm{m\,s^{-1}}$ at $t = 4\,\mathrm{s}$. Fig. 7 shows that the proposed method achieve the quick responses to both reference change and tailwind disturbance. The result also indicates the effectiveness of the thrust estimation as the maximum error is 0.42%.

V. EXPERIMENT

In this section, the proposed method was verified by experiments in the wind tunnel.

(a) (b)

(c) (d)
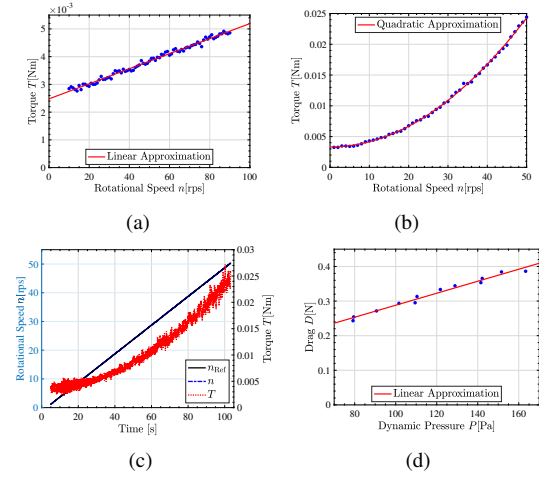
Fig. 8. (a) Measurement of B_ω and T_C. (b) $n - T$ relation with propeller at constant n. (c) Ramp response with propeller. (d) Measurement of drag of setup.

Tab. II
EXPERIMENT PARAMETERS

Parameters	Value
inertia moment of propeller J_ω	$1.29 \times 10^{-4}\mathrm{kg\,m^2}$
viscosity coefficient of motor B_ω	$4.32 \times 10^{-6}\mathrm{N\,m\,s\,rad^{-1}}$
coulomb friction of motor T_C	$2.48 \times 10^{-3}\mathrm{N\,m}$

A. Setup

Fig. 10 shows a diagram and a picture of the experimental setup. The experimental unit consists of a linear guide, a load cell, a motor, an encoder, an APC propeller 11×4, an anemometer, and a wind tunnel. The load cell measures F, the encoder measures n, and the anemometer measures V.

Before the experiment, J_ω, B_ω, and T_C are identified. As shown in Fig. 8(a), motor torque was measured at constant speeds without connecting the propeller, which determines B_ω and T_C. Then, the torque was measured with the propeller at constant n and $V = 0\,\mathrm{m\,s^{-1}}$ as shown in Fig. 8(b). Since $V = 0\,\mathrm{m\,s^{-1}}$, C_Q is constant; therefore,

$$Q \propto n^2, \tag{42}$$
$$T = (C_Q\rho D_p^5)n^2 + (2\pi B_\omega)n + T_C. \tag{43}$$

Thus, a quadratic approximation can be applied to the torque in Fig. 8(b). Finally, J_ω was calculated by measuring the torque with the propeller at $V = 0\,\mathrm{m\,s^{-1}}$ under constant acceleration command and by subtracting the result in Fig. 8(b), as shown in Fig. 8(c). Table II shows the parameters measured in the preliminary experiment.

Additionally, the drag of the experimental unit is measured and linearly approximated, assuming the drag is proportional to the dynamic pressure, as shown in Fig. 8(d). The drag on the experimental unit is subtracted from the output of the load cell.

The performance of the propeller was also tested, and the results are shown in Fig. 9(a) and Fig. 9(b).
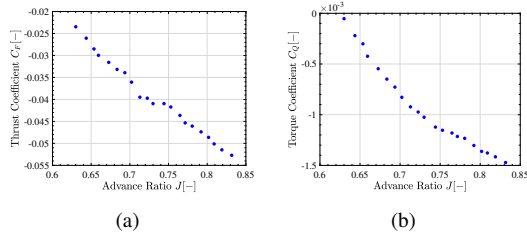
Fig. 9. (a) Thrust coefficient of test propeller. (b) Torque coefficient of test propeller.
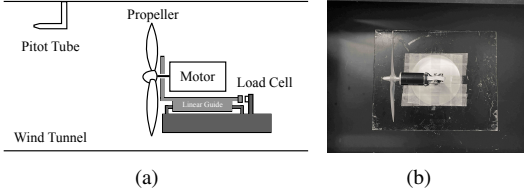
Fig. 10. (a) Diagram of experimental setup. (b) Picture of experimental setup.

Fig. 11. (a) Step response of V. (b) Step response of F.

B. Result

1) Step 1: Observer-based Airspeed Estimation: Fig. 11(a) shows the step response of V. The rotational speed of the wind tunnel fan was changed stepwise at $t = 4\,\mathrm{s}$. The time constant of the pitot tube is $1.5\,\mathrm{s}$, and that of the proposed method is $0.3\,\mathrm{s}$. The proposed method achieved five times faster estimation.

2) Step 2 & 3: Negative Thrust Control: Fig. 11(b) shows the step response of F. The thrust reference was exponentially changed from $-0.82\,\mathrm{N}$ to $-1.32\,\mathrm{N}$ at $t = 2\,\mathrm{s}$. $\hat{F}$ is the output of the observer-based thrust estimator, which is the controller feedback. F is the real value of the thrust measured by the load cell. Fig. 11(b) shows that the observer-based thrust estimator achieved accurate estimation, and the negative thrust controller achieved a quick response.

VI. CONCLUSION

EAs are attracting considerable attention as secure, efficient, and eco-friendly aviation. The electric motor enables power regeneration during descent, but keeping the desired descent angle requires the control of the thrust. In this study, the thrust control method was applied to the windmilling propeller. Also, observer-based airspeed and thrust estimation methods were proposed. The negative thrust control enables EAs to achieve more robust descent and higher followability to the target route. The simulations and experiments in the wind tunnel show the effectiveness of the methods. Future works include descent angle control by using negative thrust control and variable pitch propeller for efficiency improvement.

ACKNOWLEDGMENT

REFERENCES

[1] Akira Nishizawa, Hiroshi Kobayashi, Keiichi Okai, and Hiroshi Fujimoto. Progress of Electric Vehicle Technology and Future of Electric Aircraft. In *The 43rd JSASS Annual Meeting*, 2012.
[2] Yoichi Hori. Future vehicle driven by electricity and control - Research on four-wheel-motored "UOT Electric March II". *IEEE Transactions on Industrial Electronics*, Vol. 51, No. 5, pp. 954–962, 2004.
[3] Nicholas K. Borer, Michael D. Patterson, Jeffrey K. Viken, Mark D. Moore, JoeBen Bevirt, Alex M. Stoll, and Andrew R. Gibson. Design and Performance of the NASA SCEPTOR Distributed Electric Propulsion Flight Demonstrator. Technical report, 2016.
[4] Norihiko Adachi, Hiroshi Kobayashi, Hideaki Hakojima, and Akira Nishizawa. An Experimental Study on Energy Regeneration Using Propellers. Technical report, 2015.
[5] Kenichiro Takahashi, Hiroshi Fujimoto, Yoichi Hori, Hiroshi Kobayashi, and Akira Nishizawa. Airspeed control of electric airplane based on 2-quadrant thrust control and verification with towing test using electric vehicle. In *40th Annual Conference of the IEEE Industrial Electronics Society*, pp. 2682–2688. IEEE, 2014.
[6] Naoki Kobayashi, Hiroshi Fujimoto, and Hiroshi Kobayashi. A study of Range Extension Control System by Optimization of Motor Torque and Propeller Pitch Angle for Electric Airplane. In *IEE of Japan Technical Meeting Record*, No. 3, pp. 6–11, 2013.
[7] Nobukatsu Konishi, Hiroshi Fujimoto, Hiroshi Kobayashi, and Akira Nishizawa. Range extension control system for electric airplane with multiple motors by optimization of thrust distribution considering propellers efficiency. In *40th Annual Conference of the IEEE Industrial Electronics Society*, pp. 2847–2852. IEEE, 2014.
[8] Shota Yamada and Hiroshi Fujimoto. Precise joint torque control method for two-inertia system with backlash using load-side encoder. *IEEJ Journal of Industry Applications*, Vol. 8, No. 1, pp. 75–83, 2019.
[9] Yun Xiang, Hiroshi Fujimoto, Yoichi Hori, Yasumasa Watanabe, and Kojiro Suzuki. Proposal of Regeneration Power Control System by Optimization of Propeller Pitch Angle and Revolution Speed for Electric Airplanes. In *IEE of Japan Technical Meeting Record*, No. MEC-15-49, pp. 121–126, 2015.
[10] Masahiro Okuyama, Hiroshi Nishizawa, and Akira Kobayashi. Aerodynamic Characteristics of Windmilling on Propeller. Technical report, 2015.
[11] Akira Nishizawa, Hiroshi Kobayashi, and Hiroshi Fujimoto. Development and flight demonstration of regenerative electric propulsion system for aircraft application. In *Electric & Hybrid Aerospace Technology Symposium*, Vol. 1, Bremen Germany, 2015.
[12] Tatsuro Nodama and Shigeru Sunada. An Investigation on Battery Charging with a Propeller. *Journal of the Japan Society for Aeronautical and Space Sciences*, Vol. 63, No. 1, pp. 8–12, 2015.
[13] Yuki Hayashi, Daisuke Yashiro, Kazuhiro Yubai, and Satoshi Komada. Experimental Validation of Contact Force Control of Quadrotor Based on Rotor Angular Acceleration Control. In *019 IEEE International Conference on Mechatronics*, Vol. 1, pp. 684–689. IEEE, 2019.
[14] Barnes W. McCormick. *Aerodynamics, Aeronautics and Flight Mechanics*. John Wiley & Sons, Inc., 2nd edition, 1995.
[15] Hiroshi Kobayashi, Akira Nishizawa, and Tomoko Iijima. Airspeed estimation by electric propulsion system parameters. In *The 55st Aircraft Symposium*, pp. 869–878, 2017.
[16] APC Propellers Peformance Data. https://www.apcprop.com/technical-information/performance-data/, 2019.